ELSEVIER

Biophysical Chemistry 104 (2003) 591–603

Biophysical Chemistry

www.elsevier.com/locate/bpc

Molecular origin of the cation selectivity in OmpF porin: single channel conductances vs. free energy calculation

Christophe Danelon[a], Atsushi Suenaga[b,c], Mathias Winterhalter[a], Ichiro Yamato[c,*]

[a]*Institut de Pharmacologie et de Biologie Structurale, CNRS-UMR 5089, Universite P. Sabatier, 205 route de Narbonne, 31077 Toulouse, France*

[b]*Genomic Sciences Center, The Institute of Physical and Chemical Research (RIKEN), Yokohama 244-0804, Japan*

[c]*Department of Biological Science and Technology, Tokyo University of Science, 2641 Yamazaki, Noda-shi, Chiba 278-8510, Japan*

Received 16 February 2003; received in revised form 19 March 2003; accepted 19 March 2003

Abstract

Ion current through single outer membrane protein F (OmpF) trimers was recorded and compared to molecular dynamics simulation. Unidirectional insertion was revealed from the asymmetry in channel conductance. Single trimer conductance showed particularly high values at low symmetrical salt solution. The conductance values of various alkali metal ion solutions were proportional to the monovalent cation mobility values in the bulk phase, LiCl < NaCl < KCl < RbCl ~ CsCl, but the conductance differences were quantitatively larger than conductivity differences in bulk solutions. Selectivity measurements at low concentration showed that OmpF channels favored permeation of alkali metal ions over chloride and suggested size preference for smaller cations. These results suggest that there are specific interactions between the permeating cation and charged residues lining the channel walls. This hypothesis was supported by computational study which predicted that monovalent cations bind to Asp113 at low concentration. Here, free energy calculations revealed that the affinity of the alkali metal ions to its binding site increased with their atomic radii, $Li^+ \sim Na^+ < K^+ \sim Rb^+ \sim Cs^+$. A detailed inspection of both experimental and computational results suggested that stronger binding at the central constriction of the channel increases the translocation rate of cations under applied voltage by increasing their local concentration relative to the bulk solution.

Keywords: Free energy calculation; Ion channel; OmpF porin; Cation selectivity; Single channel conductance

1. Introduction

Ion channels play important roles in biological systems, especially in signal transduction. Malfunction of channels is the cause of many diseases and thus an important target for drugs. Despite many years of investigation several basic questions remained unsolved: ion selectivity and gating of

Abbreviations: FEP, free energy perturbation; MD, molecular dynamics.

*Corresponding author. Tel.: +81-4-7124-1501x4405; fax: +81-4-7125-1841.

E-mail address: iyamato@rs.noda.tus.ac.jp (I. Yamato).

0301-4622/03/$ - see front matter © 2003 Elsevier Science B.V. All rights reserved.
doi:10.1016/S0301-4622(03)00062-0

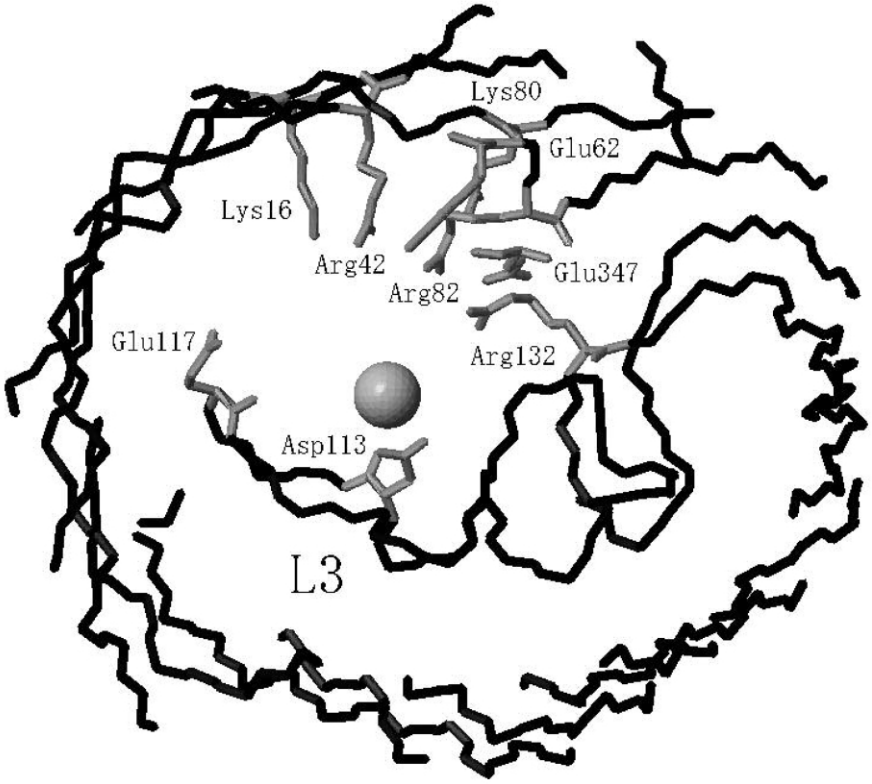

Fig. 1. Constriction zone of OmpF porin. Shown is the constriction zone ranging from 30 to 45 Å along *Z*-axis viewed from the direction perpendicular to the membrane. L3 represents the long loop which constricts the pore approximately at half-way of the barrel. Side chains of the charged residues at the constriction zone are shown in gray. A sphere represents the counter ion bound at Asp113.

channels. Recent breakthrough in X-ray high resolution crystallography enabled us to solve the structure of membrane proteins such as K^+-channel [1], Cl^--channel [2], aquaporin [3], outer membrane protein F (OmpF) porin [4], maltoporin [5] and a few others. The knowledge of the charge distribution within the channel on a molecular level has been useful to perform now more detailed molecular modeling providing more realistic information. At the same time the quality of single channel conductance could be improved and it is now tempting to compare structure and function studies to understand the mechanisms and physiological roles of the channel activities [6–8]. Recent computer simulation has been promising [9–21]. Especially, molecular dynamics (MD) simulation has provided new insights into the mechanism at atomic resolution [10,11,15–17].

One of the major components of the outer membrane proteins in *E. coli* is OmpF, which allows the permeation of hydrophilic molecules of molecular weight less than 600 Da. OmpF porin is a homo-trimer of the OmpF polypeptide with a large 16-stranded antiparallel β-barrel structure enclosing the transmembrane pore. The pore is constricted around half-way through the membrane by a long loop L3 inside the barrel (Fig. 1). The constriction zone is surrounded by clusters of positively and negatively charged amino acids; so, L3 is postulated as an electrical gate of the channel [22–24]. At low transmembrane potentials (<100 mV), the channel of the porin is open and the

current increases with the applied voltage according to Ohm's law [25]. The ion conductance is very high and the rate of ion movement was estimated to be 10^8–10^9 ions/s at 100 mV and 1 M KCl [25]. The current state of MD simulation is good enough to follow the whole ion permeation process [10,20,21].

Porins are weakly ion-selective [26] and more specifically OmpF porin is cation selective [27]. Early conductance measurements on reconstituted OmpF by Benz et al. [28] suggested that negative charges in the channel lumen were responsible for the cation preference. More recently, Asp113 was replaced by Gly and the mutated porin was four times less cation selective than the wild type [29], which suggests indeed that the Asp113 plays a role in ionic permeability [28]. However, the physical basis of its selectivity is not yet understood.

We were for the first time successful to follow the ion permeation process through OmpF porin at atomic level by computer simulation [10], demonstrating that the ion permeation proceeds by a 'push-out' mechanism rather than by simple diffusion. In this study we identified the Asp113 to be a cation binding site. Based on our previous study, we now calculated the free energy changes of binding affinities for other alkali metal ions using the cation-bound structure obtained by MD simulation [10]. In earlier studies, free energy calculations based on MD simulation (free energy perturbation; FEP) were successfully applied to estimate the changes in protein stabilities caused by mutations [30–39] and the ion selectivity of an ion channel [15]. Recent improvement in the detection of small currents through individual porins allowed us now to study in more details the ionic selectivity of OmpF channels. Here, we compared the theoretical prediction with conductance recordings on planar lipid bilayers bathing in various salt solutions differing in the alkali metal ions.

2. Experimental procedures

2.1. Materials

The following salt reagents were used: KCl and NaCl (Merck, Darmstadt, Germany), CsCl (Sigma chemical Co., St. Louis, MO), LiCl and RbCl (ABS, Basel, Switzerland). Fresh purified saline solutions were used unbuffered and had a pH of approximately 6. The lipid used was 1,2 diphytanoyl-sn-glycero-3-phosphatidylcholine (Avanti Polar-Lipids Inc.). Octyl-polyoxyethylene (Octyl-POE) detergent comes from Alexis (Lauchringen, Switzerland). The isolation and purification of OmpF was previously described [40].

2.2. Planar lipid bilayer experiments

Planar lipid bilayers were formed according to the monolayer technique of Montal and Mueller [41] across a 60 μm diameter hole in a 25 μm thick Teflon film (Goodfellow, Cambridge, UK). The film was sandwiched between two Delrine chambers, each containing 2 ml of an aqueous solution. A small magnetic stirrer was placed in each compartment in order to quickly homogenize the contents. The whole set-up was shielded from external electromagnetic fields and vibrations to minimize membrane current fluctuations. The Delrine cell was enclosed with a double isolated Faraday cage connected to the signal ground and with a home made acoustically isolating closet placed on a piezo-electric vibration isolation table model 'Elite 3' (Newport Corporation, Irvine, CA). The bilayer set-up was connected to the external circuit through a pair of Ag–AgCl electrodes via glass tubing salt bridges filled with 5% agarose soaked with 0.01 M or 0.1 M KCl (or salt) depending on the chosen buffer. The electrode in the *cis*-side of the chamber was on the ground while the other one was connected to the headstage of an Axopatch 200B amplifier (Axon Instruments, Foster City, CA) in the voltage clamp mode. Data were filtered using the low pass Bessel filter of the amplifier at 1–2 kHz and monitored with a Lecroy LT342 digital storage oscilloscope.

Membrane bilayers were obtained as previously described [42] with minor modifications. Briefly, the lipids were dissolved in a solvent mixture of *n*-hexane/chloroform (3/2, v/v). The capacity of the whole system was close to 150 pF while the residual membrane conductance (<7 pS with 1M KCl) was subtracted from the conductance measurements. The membranes were formed in a 0.01-

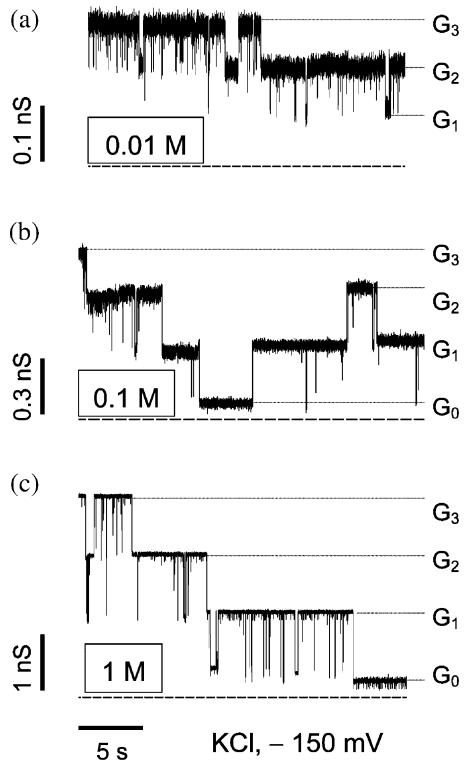

Fig. 2. Typical conductance recordings of a single OmpF protein inserted into a planar lipid bilayer at high applied voltage. Both compartments contained 0.01 M KCl (a), 0.1 M KCl (b) and 1 M KCl (c) solutions at pH approximately 6. Interruptions of the conductance by approximately one third of the initial value, G_3, correspond to single channel blockades. Occlusions are reversible events. It also demonstrates the homotrimeric form of the inserted OmpF. The fully closed porin exhibits a residual conductance, G_0, of approximately 10% of the total conductance value. The applied voltage was −150 mV. Time resolution was 0.5 ms.

M salt solution. Small amounts (~1 μl) of wild type OmpF from a 0.1 μg/ml stock solution, 1% octyl-POE detergent were injected to the *cis*-side of the chamber. Incorporation of OmpF into the bilayer was favored by applying a transmembrane voltage of 100–200 mV and by stirring for few seconds after addition. A single OmpF trimer could be stabilized into the membrane for several hours without any significant modifications of the conductance. All the experiments were made at room temperature. The applied transmembrane voltage refers to the potential of the *cis*-side minus the potential of the *trans*-side. For the various salt solutions, the electrolyte concentrations were determined from conductivity measurements using a CDM 83 conductivity meter (Radiometer, Copenhagen, Denmark).

For selectivity measurements, salt gradients were generated by adding small amounts of a concentrated solution to one side of the bilayer while the other one was maintained at a constant lower concentration. The aqueous phase was stirred few seconds and measurements were carried out after membrane potential stabilization at zero-current conditions (5–10 min). The whole titration was made on the same OmpF porin to overcome the differences that single protein measurements may be subject to. The ion selectivity was characterized by the ratio P_c/P_a (i.e. the ratio of the permeability for cations and the permeability for anions) calculated according to the theoretical Goldman–Hodgkin–Katz equation [43,44]. Zero-current membrane potentials, V_m, refer to the potential of the diluted side minus the potential of the concentrated side.

2.3. Free energy perturbation

The MD simulation does not permit to calculate absolute energies. Here in our study we were interested in free energy difference of different cations. This can be calculated in an indirect way as shown in the following schema.

$$\begin{array}{ccc} & \Delta G_A & \\ \textbf{Porin + Free ion A} & \rightarrow & \textbf{Porin·ion A} \\ \Delta G_{free} \downarrow & & \downarrow \Delta G_{complex} \\ \textbf{Porin + Free ion B} & \rightarrow & \textbf{Porin·ion B} \\ & \Delta G_B & \end{array} \quad (1)$$

where ΔG_A corresponds to the free energy difference of an ion A inside the channel with respect in free solution. ΔG_{free} stands for the free energy difference of an ion B in solution with respect to an ion A and $\Delta G_{complex}$ to the free energy difference between ion B and A in the bound state. Finally $\Delta\Delta G = (\Delta G_{complex} - \Delta G_{free})$ corresponds to

the difference between ion B and A from the solution to the bound state. For calculation of the system of Porin + Free ion (A) changing to Porin + Free ion (B) in Eq. 1, an ion (Na^+) alone was placed at the center of CAP water molecules of TIP3P [45] with radius of 25 Å. As a starting structure for porin ion (A) complex changing to Porin ion (B) complex in Eq. 1, we used the ion (Na^+) bound structure at Asp113 obtained by previous simulation [10]. Previous studies suggested that the Asp113 plays an important role in cation selectivity [10,28,29] working as a binding site. Therefore, we tried to estimate the free energy difference of binding affinities of various cations by MD simulation. In this study, we considered only one Na^+ bound to Asp113 changed to other cations. Multi-ion character of the OmpF porin channel necessitates the inclusion of the alkali metal ions locating at other sites than Asp113. But the other ions would be mobile and may take different positions. Thus, for accurate calculation, we should sample many conformations of ion positions, which makes the free energy estimation difficult under current computer power. Instead, we considered that the major contribution in the free energy difference caused by the small change of van der Waals (vdW) radius can be estimated by taking into account only one alkali metal ion bound at Asp113 as a pure model system.

CAP water molecules of TIP3P [45] with radius of 28 Å were generated at both ends and inside of the pore. Thus, the outside and inside parts of the porin were filled with water molecules. The atomic positions of all the water molecules, ions and amino acid residues at the inside surface of the pore were allowed to move, but those of the other part of the protein were fixed. A time step of 2.0 fs was used with SHAKE algorithm [46]. The temperature was kept constant at 298 K by the Berendsen coupling algorithm [47]. A constant dielectric ($\varepsilon = 1$) and cut-off distance of 20 Å were used. In the case of changing electric charges, accurate electrostatic energy estimation is necessary [36]. In our case, we changed only the vdW radius of an ion. In earlier studies modifying only the vdW radii [34–37], the calculation procedure with CAP water and cut-off method gave satisfactory results. AMBER 5.0 simulation software program [48], force field of AMBER parm94 [49] were used throughout this study.

In our modeling the parameters for Porin + Free ion and porin ion complex were energy-minimized, and MD simulations were performed to equilibrate the systems for 10.0 ps. A free energy calculation cycle using slow growth method consisted of a forward simulation ($Na^+ \rightarrow Li^+$, K^+, Rb^+ or Cs^+) for 100 ps and a reverse simulation (Li^+, K^+, Rb^+ or $Cs^+ \rightarrow Na^+$) for further 100 ps. The system was equilibrated for 10 ps at the end of the forward simulation: The root mean square fluctuation of potential energy was less than 0.4% in the all systems.

3. Results

3.1. Open-channel conductance

The ion conduction of OmpF was investigated for the series of alkali metal ions by reconstituting single OmpF trimers in planar lipid bilayers. All the conductance measurements were performed under symmetrical salt solutions. Fig. 2a–c show the conductance modifications during the spontaneous insertion of a single trimeric OmpF into a planar bilayer bathing in 0.01, 0.1 and 1 M KCl solutions, respectively. Applied high voltage generated time resolved current interruptions. A decrease of about one third of the total current demonstrates the reversible occlusion of one monomer among the three subunits of the porin [50]. Surprisingly, monomer closure was not complete leading to a residual trimer conductance, G_0, ranging from 5 to 15% of the initial OmpF conductance, G_3. The origin of G_0 is not clear yet. In the following, all the conductance values refer to the fully open-channel conductance of an individual OmpF trimer.

The Fig. 3a shows that the conductance-bulk conductivity relation appears to be linear at high concentrations. The simple extrapolation from this linear component to the *y*-intercept gives a value of approximately 0.3 nS. The channel conductance is not proportional to bulk conductivity exhibiting particularly high conductance at low concentration. For example, the OmpF conductance was only threefold reduced by a ten times dilution from 0.1

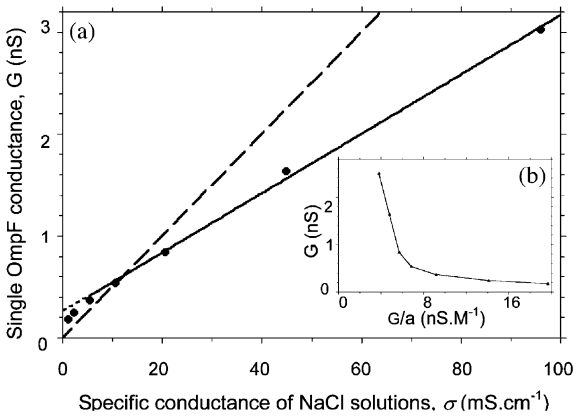

Fig. 3. (a) Single OmpF conductance as a function of specific conductance of symmetrical NaCl solutions. Applied voltage was −150 mV. The dashed line represents the estimated conductance of a single OmpF porin for free diffusion of ions through cylindrical channels (see text for details). The straight line is a linear regression at high concentrations. Its extrapolation to intercept the *y*-axis was shown in a dotted line. Solutions were unbuffered and had a pH value of approximately 6. (b) Eadie-Hofstee representation of single OmpF conductances.

M to 0.01 M NaCl solutions and 16-fold reduced by a hundred times dilution from 1 M to 0.01 M NaCl solutions, at −150 mV (Fig. 3a and Table 1).

Table 1 and Fig. 4 show that the channel conductance values for the series of alkali metal ions were qualitatively parallel to the solution conductivity values, LiCl < NaCl < KCl < RbCl ~ CsCl. However, the conductance differences were quantitatively more pronounced at low concentrations and were larger than expected from the consideration of cation mobility (Fig. 4, dashed line). The channel conductance was 2.8-fold higher from 0.01 M LiCl to 0.01 M KCl whereas the bulk conductivity of LiCl differs from KCl only by a factor of 1.3.

We found that the open-channel conductance was always higher at negative applied voltages for all investigated salt solutions (Table 1). This voltage-induced asymmetry was taken to probe the directional insertion of OmpF into the membrane. However, no correlation between the sign of the applied voltage and the orientation of the insertion

Table 1
Open-channel conductance and voltage-induced asymmetry

Salt	Concentration (M)	G^a (pS)	%[b]
LiCl	0.01	85	35
	0.1	260	22
	1	1590	<1
	0.01	175	27
NaCl	0.1	535	22
	1	2820	1
	0.01	240	39
KCl	0.1	810	27
	1	3145	2
	0.01	220	26
RbCl	0.1	850	15
	1	3650	<1
	0.01	225	36
CsCl	0.1	855	16
	1	3510	2

[a] G is the conductance of the fully open trimer. The applied voltage was −150 mV referring to the potential of the *cis*-side minus the potential of the *trans*-side.

[b] $\% = ((G^- - G^+)/G^-) \times 100$ represents the conductance asymmetry with the sign of the applied voltage where G^- and G^+ stand for the conductance at −150 and +150 mV, respectively. The data represent the mean of at least four independent experiments. The S.D. was always <15% of the mean value.

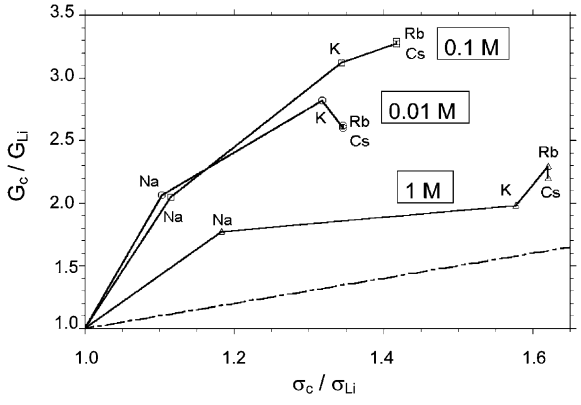

Fig. 4. Single OmpF protein conductance for various solutions differing in the alkali metal ions relative to the conductance of LiCl containing aqueous phase vs. the ratio of their respective bulk conductivity. Symmetrical salt concentrations were 0.01 M (circles), 0.1 M (squares) and 1 M (triangles). The dashed line is from the assumption that the conductance differences between the series of alkali metal ions equal the bulk conductivity differences.

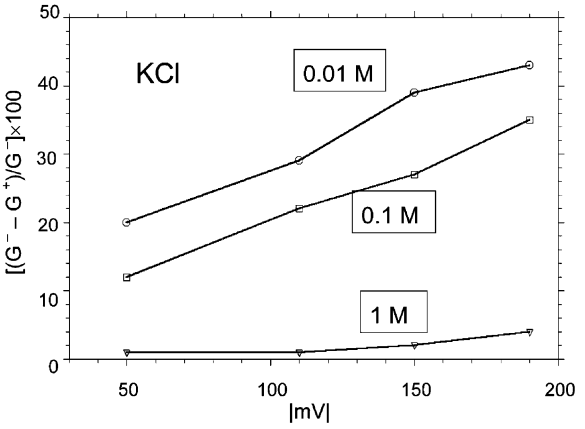

Fig. 5. Open-channel conductance asymmetry (in percent) with the sign of the applied voltage vs. the absolute voltage values under symmetrical 0.01 M KCl (circles), 0.1 M KCl (squares) and 1 M KCl (triangles) salt solutions. G^- and G^+ are the OmpF conductance at negative and positive voltages, respectively.

was observed. Table 1 and Fig. 5 show that the ion transport asymmetry was more pronounced at high voltage and low ionic strength. Between + 190 and −190 mV the conductance difference dropped from 43% at 0.01 M to 4% at 1 M KCl solutions.

3.2. Ion selectivity

The selectivity of OmpF porin was determined by measuring the zero-current membrane potentials produced by salt gradients across the channels. The vectorial insertion of single OmpF porin into the bilayer permitted to control the direction of the concentration gradient generated across the channels (from *cis* to *trans*-side or the opposite). Two series of concentration gradients, at low then at high salt concentrations, were performed on individual incorporated OmpF porins as illustrated in Fig. 6. The derived selectivity coefficients showed no significant difference with the direction of the concentration gradient. The mean values of the permeability ratios of the alkali metal ions over the chloride ion are reported in Table 2. The results corroborate the cation-selectivity of the OmpF porin and show that channel selectivity decreases along the sequence of the electrolytes LiCl, NaCl, KCl, RbCl, CsCl. At low concentration, the OmpF porin was highly cation-selective with $P^+_{Li}/P^-_{Cl}=37.0$ vs. only 4.6 at high salt concentration.

3.3. MD simulation

The calculated free energy changes for the different cation bindings are summarized in Table 3. The larger negative value of free energy change ($\Delta\Delta G$) for Cs^+, Rb^+ or K^+ than Na^+ and Li^+ indicates a higher binding affinity to the Asp113. We found in our simulation that the ions bound at Asp113 had two water molecules less than the corresponding free ions; free Li^+ was surrounded with 5 water molecules and lost two when bound and free Cs^+ was surrounded with 10 water molecules and lost two when bound. Even though

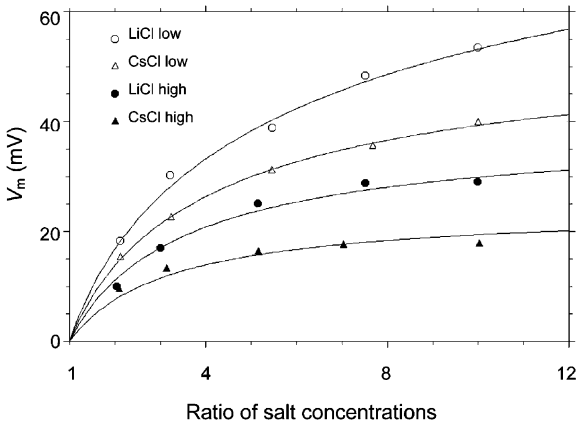

Fig. 6. Plot of the zero-current membrane potentials vs. the ratio of the salt concentrations on both compartments for LiCl and CsCl solutions. Membrane formation and OmpF porin insertions were performed in 0.01-M salt solution to both compartments. For the low concentration experiments, the lower concentrated side of the bilayer moiety was maintained at 0.01 M whereas the concentration on the other side raised to 0.1 M by adding increasing amounts of a 3 M stock solution. For the high concentration experiments, the lower concentrated side of the bilayer moiety was maintained at 0.1 M whereas the concentration on the other side was increased up to 1 M. These experimental procedures lead to identical concentration ratios but the number of ions in solution is different. The V_m values correspond to the mean of at least four independent experiments. The curves were fitted to the theoretical Goldman–Hodgkin–Katz equation. The salt concentrations were used unbuffered and had a pH approximately 6.

the permeation of cations through the water-filled OmpF channels does not require its complete dehydration, a partial reduction of the hydration shell is expected to be a crucial step of the association rate to Asp113 (even for Li^+ which strongly interacts with the water molecules of the aqueous phase).

4. Discussion

To gain insight into the molecular basis for ion selectivity of the general diffusion porin OmpF, we performed a combination of electrophysiological recordings and MD simulation. Our open-channel conductance and selectivity studies at the single protein level clearly demonstrated the active role of the channel lumen during the ion transport. Correlating conduction properties and structural aspects highlighted by MD simulation is essential to understand the physics involved in the ion translocation.

4.1. The ion transport through OmpF channel is not a simple diffusion process

The open-channel conductance of OmpF porin was studied in symmetrical solutions of the series LiCl–NaCl–KCl–RbCl–CsCl. Fig. 3a showed that the channel conductance was not a linear function of the bulk conductivity demonstrating that OmpF channel plays a specific role in the ion transport (compared to free diffusion of ions inside an inert water-filled pore). The estimated conductance of a single OmpF molecule for free diffusion of ions through cylindrical channels is shown in Fig. 3a (dashed line). With this assumption, the channel conductance can be expressed as:

$$G_{\mathrm{diff}} = \sigma\left[\left(f_c \pi R_{\mathrm{eff}}^2 / L\right)^{-1} + \left(2R_{\mathrm{eff}}\right)^{-1}\right]^{-1}, \qquad (2)$$

where R_{eff} is the effective radius of an OmpF pore directly determined from the crystal structure, L is the channel length, σ is the bulk conductivity and f_c is the Faxen correction factor which takes into account frictional interactions between the permeant solvated ions and the channel walls [51]; the first term is the resistance of the cylindrical pore and the second term is the sum of the access resistance from each side of the channel [44]. For $R_{\mathrm{eff}} = 0.7$ nm [50], $L = 4$ nm and $f_c = 0.5$ (corresponding to a ratio of solvated ions to channel effective radius of 0.25), we obtain $G_{\mathrm{diff}} = 50\sigma$ (with G_{diff} in pS and σ in mS/cm) as an estimation of the OmpF trimer conductance for passive ionic transport. It is interesting to note that at symmet-

Table 3
Summary of free energy analysis

Process	$\Delta\Delta G$ (kcal/mol)
$Na^+ \rightarrow Li^+$	$+0.007 \pm 0.607$
$Na^+ \rightarrow K^+$	-1.148 ± 0.223
$Na^+ \rightarrow Rb^+$	-1.295 ± 0.386
$Na^+ \rightarrow Cs^+$	-1.350 ± 0.312

Table 2
Zero-current membrane potentials V_m and derivated permeability ratios of the alkali metal ions and chloride anion at low and high salt concentrations

Salt	Pauling cation radius (Å)	Low concentrations		High concentrations	
		V_m (mV)[a]	P_c/P_a[b]	V_m (mV)[c]	P_c/P_a
LiCl	0.68	55 ± 6	37.0 ± 5.0	30 ± 3	4.5 ± 1.0
NaCl	0.97	48 ± 2	19.0 ± 2.5	30 ± 3	4.5 ± 1.0
KCl	1.33	46 ± 3	15.5 ± 2.5	25 ± 4	3.5 ± 0.5
RbCl	1.47	42 ± 3	10.5 ± 2.0	22 ± 3	3.0 ± 0.5
CsCl	1.67	40 ± 4	8.5 ± 1.5	19 ± 2	3.0 ± 0.5

[a] Here, the V_m values were measured at 0.01 M/0.1 M condition.
[b] The selectivity values P_c/P_a were obtained by fitting the experimental V_m's determined for five increasing concentration gradients with the theoretical Goldman–Hodgkin–Katz equation (Fig. 6). The zero-current membrane potentials V_m refer to the less concentrated side potential minus the more concentrated side potential. Each value is the mean of at least four independent experiments.
[c] Here, the V_m values were measured at 0.1 M/1 M condition.

rical 0.01 M NaCl solution, the experimental open-channel conductance $G_{exp} \sim 3\ G_{diff,}$ indicating that the OmpF channel enhances the conducting properties, whereas at 1 M NaCl $G_{exp} \sim 0.6\ G_{diff,}$ suggesting that free diffusion would be more efficient at high salt concentration, which corresponds to the observation by MD simulation [20,21].

4.2. The permeating cations interact with specific elements along the ionic pathway

At low concentration where the OmpF channel has been found to be strongly cation selective, the cations are expected to mainly contribute to the channel conductance. According to the Gouy-Chapman theory, the large conductance value may reflect an increase of the local cation concentration inside the channel due to negative surface charges distributed on the pore walls. Assuming the OmpF channels as perfect cylinders with the geometrical parameters described above, the negative surface potential, ϕ, generated by negative point charges, q, is given by [52,53]:

$$\phi = 2q\exp\left(-R_{eff}/\lambda_D\right)/(4\pi R_{eff}\varepsilon\varepsilon_0), \quad (3)$$

where ε_0 ($=8.85\times10^{-12}$ F/m) and ε ($=80$) are the absolute dielectric constant of vacuum and the relative dielectric constant of water, respectively, and λ_D is the Debye length for monovalent electrolyte. The OmpF conductance, G^*, corrected by the increased cation concentration near the negative charges is given by:

$$G^* = G\exp(\phi F/(RT)). \quad (4)$$

Logarithmic plot of G^* vs. the cation concentration in the aqueous phase should not show any dependence on the species of the alkali metal ions taking into account the same negative point charge value. However, the differences between G^* and G values clearly depended on the species of the alkali metal ions (data not shown). Another approach based on a simplified form of the Gouy-Chapman theory [54] plotting the channel conductance values against the square root of the bulk conductivity did not permit to derive the conclusion of pure electrostatic interactions between the surface charges of the pore and the alkali metal ions (data not shown). Such a finding suggests that we have to consider the specific physicochemical properties of the cations, not only the charge but also hydration energy, hydrated radius and so on.

Furthermore, Fig. 4 showed that the conductance differences along the alkali metal ion series cannot be understood in terms of bulk solution conductivity differences. The mobility of ions inside the channel is not the only parameter controlling the channel conductance confirming the contribution of other cation specific factors. Together with the above electrostatic considerations, we argue that the permeating cations specifically interact with lateral charges pointing toward the channel lumen. This result is in agreement with our MD simulation at low salt concentration which revealed the presence of such a binding site positioned at Asp113. In this sense, our study is complementary to the studies of Im and Roux [20,21], especially focusing at the condition of low salt concentration; they [21] observed specifically high cation conductance compared to anion conductance at 0.01 M concentration.

The complex conductance–activity relationship, deviation from a simple Michaelis–Menten kinetics and biphasic curve of the Eadie–Hofstee representation (Fig. 3b), is in favor of a multi-occupancy channel model which is consistent with the ‘push-out’ mechanism of cation conduction observed by a previous computational study [10]. Recent MD simulation with multiple free ions inside the pore showed that ions can pass freely through the constriction zone probably because most charges are screened by counter-ions [20]. Moreover, counter-ions placed near charged residues arranged along the pore reduce the effective radius of the channel by steric hindrance ($R_{eff} < 0.7$ nm) which is in agreement with the lower experimental conductance at high concentrations comparing with a passive channel of $R_{eff} =$ 0.7 nm (Fig. 3a).

The unidirectional orientation of the OmpF porin probably originates from its structural asymmetry. Similar directional insertion was reported for the specific maltoporin channels [7,51], suggesting an similar incorporation process. It is seen

that the transport of ions through the OmpF channel is strong function of both applied voltage and ionic strength (Fig. 5). Similar observations for maltose and maltoporin [51] and for ampicillin and OmpF [8] were tentatively explained by field-induced changes in binding to specific site. This analysis is consistent with specific interactions between cations and the pore wall. An electromechanical coupling between the external field and charges inside the channel may modify the specific interactions between the permeating ions and charged residues positioned along the ionic pathway. It is noteworthy that the main ion transport properties, i.e. the conductance–concentration relationship and the magnitude of ionic screening could be reproduced by Brownian dynamics and Poisson–Nernst–Planck electrodiffusion theory [21]. Their results were in excellent agreement with our experimental results.

4.3. Single channel recordings vs. free energy calculation

For a better understanding of the molecular mechanism involved during the cation transport through OmpF channel we combined the conductance in the low concentration regime and the free energy changes for the various alkali metal ions.

The ions passing through the OmpF channels may encounter several potential barriers and we found by MD simulation that Asp113 is the strongest binding site for a permeant cation at low salt concentration [10]. Therefore, it is reasonable that the energetics of a permeant cation is governed by a simple one site two-barrier model [55,56] where the energy well would be located at Asp113 and the corresponding rate constants of cation binding would be characteristic of the whole permeation process. In our simulation the cations bound at Asp113 lost two water molecules from the hydration of the free ions. The lyotropic series of alkali metal ions corresponds to the order of magnitude of hydration energy, $Li^+ > Na^+ > K^+ > Rb^+ > Cs^+$ [44], which determines the binding affinity to cation exchange resins, and expectedly to a carboxylic amino acid, Asp in this study (Table 3). Thus, Cs^+ easily loses its hydration water and binds to Asp113 with higher affinity. It is seen that cation mobility alone cannot explain the conductance differences for the various salt solutions (Fig. 4). Combining the experimental data, stronger binding of a larger cation correlated with increasing channel conductance. This result supports that a deep energy well increases the translocation rate by increasing the local cation concentration inside the channel: Cs^+ is bound with higher affinity, increasing the Cs^+ local concentration at the constriction zone, which enhances the conductance specifically more than for the case of Li^+. This participation of bound cations in the conductance may be enabled by the 'push-out' mechanism as was observed in MD simulation [10].

Free energy difference between Na^+ and Li^+ (Table 3) was very small, while the difference of conductance values (Table 1) or hydration energies [44] was significant (Table 1). We do not have good explanation for this discrepancy. On the other hand, the free energy difference between Na^+ and the group of K^+, Rb^+ and Cs^+ corresponded semi-quantitatively well to the difference of conductance or hydration energies. In this sense, we can rely on the results of the free energy calculation.

Our computational study also suggests an explanation for the cation selectivity reduction along the series LiCl, NaCl, KCl, RbCl, CsCl. Stronger bound cations, on the one hand, exert the steric hindrance effect working as inert chemical species for permeation and, on the other hand, give the higher screening probability of the negative charge at Asp113 modulating the energy profile inside the channel by decreasing the electrostatic repulsion for permeating anions. As a consequence the cation selectivity is lower for tightly bound alkali metal ions. Similar results were reported for the reversible binding of halide anions to the Roflamycoin channel [57]. The decrease of the ionic selectivity coefficient, P_c/P_a, at high concentrations (Table 2) can be qualitatively explained by an increase of ionic screening of the negative electrostatic potential arising from the charges into the pore. Recently, mutation of basic residues has been shown to result in increase of cation selectivity [17]. Note that the charge selectivity and the zero-current potential (V_m) determined at high NaCl

concentrations (Table 2) gave similar results as previous data [29,58] obtained under identical experimental conditions but performed on multi-channels inserted into the bilayer. However, the results slightly differ from those obtained previously by Benz et al. [27,59]. One reason for the discrepancy may originate from using solvent containing membranes which results in less stressed proteins.

5. Conclusions

We explored the molecular mechanism of ion transport through the general diffusion OmpF protein. Analysis of single channel recordings of individual OmpF trimers inserted into planar lipid bilayers unveiled new features of ion conduction properties. Charge selectivity and salt concentration-dependence of the open-channel conductance for the series of alkali metal ions demonstrated unambiguously that the water-filled pore is not passive for ion transport. Solid evidences for specific interactions between the permeating cations and the channel walls were reported: (1) deviation from a simple point charge theory, (2) large conductance differences compared to the differences of cation mobility in the aqueous solution, (3) strong effect of the applied voltage on ion conduction. These experimental data are compatible with the identification by MD simulation of Asp113 as binding site for cations at low concentration. Free energy calculations showed that the affinity for Cs^+, Rb^+ or K^+ to Asp113 is higher than Na^+ and Li^+ which is consistent with physicochemical data of hydration energy for the alkali metal ions. Combining our experimental and computational data revealed that a deep energy trap is functionally important for segregation of larger alkali metal ions inside the channel thus enhancing the translocation rate under applied voltage at low concentration. Our results also indicated that strong cation binding was accompanied by higher anion permeability. In the future, combination of experiments and MD simulation can be applied to gain insight in the voltage-induced charge rearrangements along the ion pathway and also in the molecular mechanism of channel gating.

Acknowledgments

This work was supported (to I. Y.) by Grant-in-Aid for Scientific Research on Priority Area (C) Genome Information Science from the Ministry of Education, Culture, Sports, Science and Technology of Japan. We would like to thank Prof. J.P. Rosenbusch for initiating this work and Dr Ekaterina M. Nestorovich and Prof. Roland Benz for helpful discussion.

References

[1] D.A. Doyle, J.M. Cabral, R.A. Pfuetzner, et al., The structure of the potassium channel: molecular basis of K+ conduction and selectivity, Science 280 (1998) 69–77.
[2] R. Dutzler, E.B. Campbell, M. Cadene, B.T. Chait, R. MacKinnon, X-ray structure of a ClC chloride channel at 3.0 A reveals the molecular basis of anion selectivity, Nature 415 (2002) 287–294.
[3] K. Murata, K. Mitsuoka, T. Hirai, et al., Structural determinants of water permeation through aquaporin-1, Nature 407 (2000) 599–605.
[4] S.W. Cowan, T. Schirmer, G. Rummel, et al., Crystal structures explain functional properties of two *E. coli* porins, Nature 358 (1992) 727–733.
[5] T. Schirmer, T.A. Keller, Y.F. Wang, J.P. Rosenbusch, Structural basis for sugar translocation through maltoporin channels at 3.1 A resolution, Science 267 (1995) 512–514.
[6] S.M. Bezrukov, L. Kullman, M. Winterhalter, Probing sugar translocation through maltoporin at the single channel level, FEBS Lett. 476 (2000) 224–228.
[7] L. Kullman, M. Winterhalter, S.M. Bezrukov, Transport of maltodextrins through maltoporin: a single-channel study, Biophys. J. 82 (2002) 803–812.
[8] E.M. Nestorovich, C. Danelon, M. Winterhalter, S.M. Bezrukov, Designed to penetrate: time-resolved interaction of single antibiotic molecules with bacterial pores, Proc. Natl. Acad. Sci. USA 99 (2002) 9789–9794.
[9] A. Suenaga, I. Yamato, M. Saito, Progress in cell research, in: M. Sokabe, A. Auerbach, F. Sigworth (Eds.), Towards Molecular Biophysics of Ion Channels, vol. 6, Elsevier Sci. Pub, Amsterdam, 1997, pp. 217–232.
[10] A. Suenaga, Y. Komeiji, M. Uebayasi, T. Meguro, M. Saito, I. Yamato, Computational observation of an ion permeation through a channel protein, Biosci. Rep. 18 (1998) 39–47.
[11] D.P. Tieleman, H.J.C. Berendsen, A molecular dynamics study of the pores formed by *Escherichia coli* OmpF porin in a fully hydrated palmitoyloleoylphosphatidylcholine bilayer, Biophys. J. 74 (1998) 2786–2801.

[12] L. Guidoni, V. Torre, P. Carloni, Potassium and sodium binding to the outer mouth of the K+ channel, Biochemistry 38 (1999) 8599–8604.
[13] T.W. Allen, S. Kuyucak, S.H. Chung, Molecular dynamics study of the KcsA potassium channel, Biophys. J. 77 (1999) 2502–2516.
[14] I.H. Shrivastava, M.S. Sansom, Simulations of ion permeation through a potassium channel: molecular dynamics of KcsA in a phospholipid bilayer, Biophys. J. 78 (2000) 557–570.
[15] J. Åqvist, V. Luzhkov, Ion permeation mechanism of the potassium channel, Nature 404 (2000) 881–884.
[16] S. Berneche, B. Roux, Molecular dynamics of the KcsA K(+) channel in a bilayer membrane, Biophys. J. 78 (2000) 2900–2917.
[17] B. Roux, W. Im, Ion channels, permeation, and electrostatics: insight into the function of KcsA, Biochemistry 39 (2000) 13295–13306.
[18] F. Zhu, E. Tajkhorshid, K. Schulten, Molecular dynamics study of aquaporin-1 water channel in a lipid bilayer, FEBS Lett. 504 (2001) 212–218.
[19] B.L.D. Groot, H. Grubmüller, Water permeation across biological membranes: mechanism and dynamics of aquaporin-1 and GlpF, Science 294 (2001) 2353–2357.
[20] W. Im, B. Roux, Ions and counterions in a biological channel: a molecular dynamics simulation of OmpF porin from *Escherichia coli* in an explicit membrane with 1 M KCl aqueous salt solution, J. Mol. Biol. 319 (2002) 1177–1197.
[21] W. Im, B. Roux, Ion permeation and selectivity of OmpF porin: a theoretical study based on molecular dynamics, Brownian dynamics, and continuum electrodiffusion theory, J. Mol. Biol. 322 (2002) 851–869.
[22] S.A. Benson, J.L.L. Occi, B.A. Sampson, Mutations that alter the pore function of the OmpF porin of *Escherichia coli* K12, J. Mol. Biol. 203 (1988) 961–970.
[23] R. Misra, S.A. Benson, Genetic identification of the pore domain of the OmpC porin of *Escherichia coli* K-12, J. Bacteriol. 170 (1988) 3611–3617.
[24] K.-L. Lou, N. Saint, A. Prilipov, et al., Structural and functional characterization of OmpF porin mutants selected for larger pore size. I. Crystallographic analysis, J. Biol. Chem. 271 (1996) 20669–20675.
[25] H. Schindler, J.P. Rosenbusch, Matrix protein in planar membranes: clusters of channels in a native environment and their functional reassembly, Proc. Natl. Acad. Sci. USA 78 (1981) 2302–2306.
[26] R.E.W. Hancock, Role of porins in outer membrane permeability, J. Bacteriol. 169 (1987) 929–933.
[27] R. Benz, A. Schmid, R.E.W. Hancock, Ion selectivity of gram-negative bacterial porins, J. Bacteriol. 162 (1985) 722–727.
[28] R. Benz, K. Janko, W. Boos, P. Läuger, Formation of large, ion-permeable membrane channels by the matrix protein (porin) of *Escherichia coli*, Biochim. Biophys. Acta 511 (1978) 305–319.
[29] N. Saint, K.-L. Lou, C. Widmer, M. Luckey, T. Schirmer, J.P. Rosenbusch, Structural and functional characterization of OmpF porin mutants selected for larger pore size. II. Functional characterization, J. Biol. Chem. 271 (1996) 20676–20680.
[30] L. Dang, K.J. Merz, P.A. Kollman, Free energy calculations on protein stability: Thr-157 → Val-157 mutation of T4 lysozyme, J. Am. Chem. Soc. 111 (1989) 8505–8508.
[31] J. Gao, K. Kuczera, B. Tidor, M. Karplus, Hidden thermodynamics of mutant proteins: a molecular dynamics analysis, Science 244 (1989) 1069–1072.
[32] M. Prevost, S.J. Wodak, B. Tidor, M. Karplus, Contribution of the hydrophobic effect to protein stability: analysis based on simulations of the Ile-96-Ala mutation in barnase, Proc. Natl. Acad. Sci. USA 88 (1991) 10880–10884.
[33] D. Mendel, J.A. Ellman, Z. Chang, D.L. Veenstra, P.A. Kollman, P.G. Schultz, Probing protein stability with unnatural amino acids, Science 256 (1992) 1798–1802.
[34] Y. Komeiji, M. Uebayasi, J. Someya, I. Yamato, Free energy perturbation study on a Trp-binding mutant (Ser88 → Cys) of the trp-repressor, Prot. Eng. 5 (1992) 759–767.
[35] Y. Komeiji, I. Fujita, N. Honda, M. Tsutsui, T. Tamura, I. Yamato, Glycine 85 of the trp-repressor of *E. coli* is important in forming the hydrophobic tryptophan binding pocket; experimental and computational approaches, Prot. Eng. 7 (1994) 1239–1247.
[36] M. Saito, Molecular dynamics/free energy study of a protein in solution with all degrees of freedom and long-range Coulomb interactions, J. Phys. Chem. 99 (1995) 17043–17048.
[37] N. Honda, Y. Komeiji, M. Uebayasi, I. Yamato, Computational design of a substrate specificity mutant of a protein, Proteins 26 (1996) 459–464.
[38] Y. Sugita, A. Kitao, Improved protein free energy calculation by more accurate treatment of nonbonded energy: application to chymotrypsin inhibitor 2, V57A, Proteins 30 (1998) 388–400.
[39] H. Kono, M. Saito, A. Sarai, Stability analysis for the cavity-filling mutations of the Myb DNA-binding domain utilizing free-energy calculations, Proteins 38 (2000) 197–209.
[40] R.M. Garavito, J.P. Rosenbusch, Isolation and crystallization of bacterial porin, Methods Enzymol. 125 (1986) 309–328.
[41] M. Montal, P. Mueller, Formation of bimolecular membranes from lipid monolayers and a study of their electrical properties, Proc. Natl. Acad. Sci. USA 69 (1972) 3561–3566.
[42] M. Winterhalter, Sugar transport through channels reconstituted in planar lipid membranes, Colloid Surface A 149 (1999) 547–551.
[43] A.L. Hodgkin, B. Katz, The effect of sodium ions on the electrical activity of the giant axon of the squid, J. Physiol. (Lond.) 108 (1949) 37–77.

[44] B. Hille, Ionic Channels of Excitable Membranes, second ed., Sinauer Associates Inc, Sunderland, Massachusetts, 1992.
[45] W.L. Jorgensen, J. Chandrasekhar, J.D. Madura, R.W. Impey, M.L. Klein, Comparison of simple potential functions for simulating liquid water, J. Chem. Phys. 79 (1983) 926–935.
[46] J.-P. Ryckaert, B. Ciccotti, H.J.C. Berendsen, Numerical integration of the cartesian equations of motion of a system with constraints: molecular dynamics of *n*-alkanes, J. Comput. Phys. 23 (1977) 327–341.
[47] H.J.C. Berendsen, J.P.M. Postma, W.F. van Gunsteren, A. DiNola, J.R. Haak, Molecular dynamics with coupling to an external bath, J. Chem. Phys. 81 (1984) 3684–3690.
[48] D.A. Case, D.A. Pearlman, J.W. Caldwell, et al., AMBER 5.0, University of California, San Francisco, 1997.
[49] W.D. Cornell, P. Cieplak, C.I. Bayly, et al., A second generation force field for the simulation of proteins, nucleic acids, and organic molecules, J. Am. Chem. Soc. 117 (1995) 5179–5197.
[50] T.K. Rostovtseva, E.M. Nestorovich, S.M. Bezrukov, Partitioning of differently sized poly(ethylene glycol)s into OmpF porin, Biophys. J. 82 (2002) 160–169.
[51] S.M. Bezrukov, Ion channels as molecular coulter counters to probe metabolite transport, J. Membrane Biol. 174 (2000) 1–13.
[52] A.P. Nelson, D.A. McQuarrie, The effect of discrete charges on the electrical properties of a membrane, J. Theor. Biol. 55 (1975) 13–27.
[53] J. Trias, R. Benz, Characterization of the channel formed by the mycobacterial porin in lipid bilayer membranes. Demonstration of voltage gating and of negative point charges at the channel mouth, J. Biol. Chem. 268 (1993) 6234–6240.
[54] G. Menestrina, R. Antolini, Ion transport through hemocyanin channels in oxidized cholesterol artificial bilayer membranes, Biochim. Biophys. Acta 643 (1981) 616–625.
[55] I. Yamato, Ordered binding model as a general tight coupling mechanism for bioenergy transduction—A hypothesis, Proc. Jpn. Acad. 69 (1993) 218–223.
[56] P. Läuger, Ion transport through pores: a rate-theory analysis, Biochim. Biophys. Acta 311 (1973) 423–441.
[57] P.A. Grigorjev, S.M. Bezrukov, Hofmeister effect in ion transport: reversible binding of halide anions to the roflamycoin channel, Biophys. J. 67 (1994) 2265–2271.
[58] P.S. Phale, A. Philippsen, C. Widmer, V.P. Phale, J.P. Rosenbusch, T. Schirmer, Role of charged residues at the OmpF porin channel constriction probed by mutagenesis and simulation, Biochemistry 40 (2001) 6319–6325.
[59] R. Benz, K. Janko, P. Läuger, Ionic selectivity of pores formed by the matrix protein (porin) of *Escherichia coli*, Biochim. Biophys. Acta 551 (1979) 238–247.